Electronic Supplementary Material (ESI) for Chemical Communications.
This journal is © The Royal Society of Chemistry 2020

Fe doped Co_3O_4 polycrystalline nanosheets as binder-free bifunctional cathode for robust and efficient Zinc-air batteries

Xiao-Zhi Liu,†[a,b] *Tang Tang,*†[b,c] *Wen-Jie Jiang,**[c] *Qing-Hua Zhang,*[a] *Lin Gu**[a,b,d] *and Jin-Song Hu**[b,c]

a. *Beijing National Laboratory for Condensed Matter Physics, Institute of Physics, Chinese Academy of Sciences, Beijing 100190, China. Email: l.gu@iphy.ac.cn*

b. *University of Chinese Academy of Sciences, Beijing 100049, China.*

c. *Beijing National Laboratory for Molecular Sciences (BNLMS), CAS Key Laboratory of Molecular Nanostructure and Nanotechnology, Institute of Chemistry, Chinese Academy of Sciences (CAS), Beijing 100190, China. Email: jiangwenjie@iccas.ac.cn; hujs@iccas.ac.cn*

d. *Songshan Lake Materials Laboratory, Dongguan 523808, China.*

†. *The authors contributed equally.*

This file includes Fig. S1-S12 and Table S1-S3

Experimental Section

Chemicals and Materials: $Fe_2(NO_3)_3 \cdot 9H_2O$ (98%), $CoNO_3 \cdot 6H_2O$ (98%), Iridium (IV) oxide (99.99%), 20% Pt/C, potassium hydroxide (99.98%), hexamethylenetetramine ($C_6H_{12}N_4$) were purchased from Alfa Aesar. Ethanol, ammonia aqueous solution (25-28%), and hydrochloric acid were obtained from Beijing Chemical Work in analytic grade (A.R.). Carbon cloth (CC) was purchased from Wuhan Instrument (Wuhan) and cut into 4 cm × 3 cm in size for further use. To remove impurities on the surface, the carbon cloth was carefully cleaned with concentrated HNO_3 under 120 ^oC for 3 h and washed with water until the pH reached 7. All chemicals were used as received without any further purification. Milli-Q ultrapure water (resistance of 18.2 MΩ·cm at 25 °C) was used for all experiments.

Synthesis of Co LDH@CC and CoFe LDH@CC precursor: In a typical procedure, a mixture of 4 mmol cobalt acetate and 500 mg hexamethylenetetramine (HMTA) were dissolved in 30 mL methanol under continuous stirring to obtain a clear solution. The mixed solution was then transferred into a 50 mL Teflon stainless-steel autoclave with a piece of cleaned carbon cloth substrate (4 cm × 3 cm in size) immersed in the solution. The autoclave was locked tightly and maintained in an electric oven at 120 ^oC for 8h and then naturally cooled down to room temperature. The as-obtained sample was then washed with ethanol three times and dried naturally to achieve the Co layered double hydroxides (Co LDH). The CoFe LDH was synthesized using the same method except for changing the type of metal salt (3 mmol $CoNO_3$ and 1 mmol $Fe_2(NO_3)_3$) while keeping the total amount as 4 mmol.

Synthesis of Co_3O_4@CC and Fe-doped Co_3O_4@**CC:** The achieved Co LDH and CoFe LDH were annealed at 300 ^oC for 2h in the air atmosphere to achieve the Co_3O_4 and Fe-doped Co_3O_4.

Material Characterization: The powder X-ray diffraction patterns (XRD) of the samples were recorded at a scan rate of 5° min^{-1} on a diffractometer (Rigaku D/max 2500) with Cu Kα radiation (λ = 1.54056 Å). The powders for XRD examination were removed from the as-prepared samples by intense ultrasonic treatment. The morphologies and structural details of the samples were observed using a Hitachi S-4800 field emission scanning electron microscope (FESEM) (15 kV & 10 mA) and transmission electron microscope (TEM, Thermo Fisher Scientific, Tecnai G2 F20) operating at 200 kV. Elemental mapping was performed with an energy dispersive spectrometer (EDS) system (Oxford Materials Analysis) equipped on the TEM. The Fe doping concentration was obtained using an inductively coupled plasma optical emission spectrometer (ICP-OES, Agilent 730, USA). X-ray photoelectron spectroscopy (XPS) measurements were performed on an ESCALab 250Xi (Thermo Fisher Scientific) with Mg K radiation.

Electrochemical measurements: All electrocatalytic measurements were performed at room temperature on an Autolab PGSTAT302N electrochemical workstation (Metrohm, Netherlands) using a conventional three-electrode configuration in 0.1 M KOH aqueous solution. The Co_3O_4@CC and Fe-Co_3O_4@CC were directly used as the working electrodes. A carbon rod and Ag/AgCl electrode were used as the counter electrode and the reference electrode, respectively. For OER measurements, linear sweep voltammetry (LSV) polarization curves were recorded at a scan rate of 5 mV s^{-1} with 90% iR-compensation unless specifically indicated. Electrochemical impedance spectroscopy (EIS) was conducted at a potential of 1.465 V (*vs*. RHE) in the frequency range of 100 kHz to 10 mHz. The double-layer capacitances (C_{dl}) of the catalysts were measured in the potential range without faradaic processes at various scan rates including 120, 100, 80, and 60 mV s^{-1} in 1 M KOH. For ORR, the linear sweep voltammetry (LSV) polarization curves were recorded at a scan rate of 10 mV s^{-1} without iR-compensation. All potentials reported in this work were referenced to the reversible hydrogen electrode (RHE), which were converted according to the following equation:

$$E_{\mathrm{RHE}} = E_{\mathrm{Ag/AgCl}} + 0.098 + 0.059 \times \mathrm{pH}$$

where $E_{Ag/AgCl}$ is the measured potential.

Zn-air battery measurements: The Zn-air battery measurements were performed using a homemade Zn-air device. A polished Zn plate was used as the anode. For the air cathode, the gas diffusion layer (GDL) was prepared by hot-pressing (80 $^{\circ}$C for 90 s) the carbon cloth with catalysts array on it with a waterproof breathable film. A mixed solution of 0.2 M $ZnCl_2$ + 6 M KOH was used as the electrolyte. A gas diffusion hole on the air cathode allows O_2 from ambient air to reach the catalyst layer. A Pt/C +IrO_2 mixed catalysts with a Pt/Ir atomic ratio of ~ 50% was used as control. The discharge and charge curves were recorded at a scan rate of 5 mV s^{-1}. The cycling measurements were recorded on a battery device with an electrolyte circulating setup at a discharge and charge current density of 2 mA cm^{-2}. Each discharge/charge period was set to be 10 min.

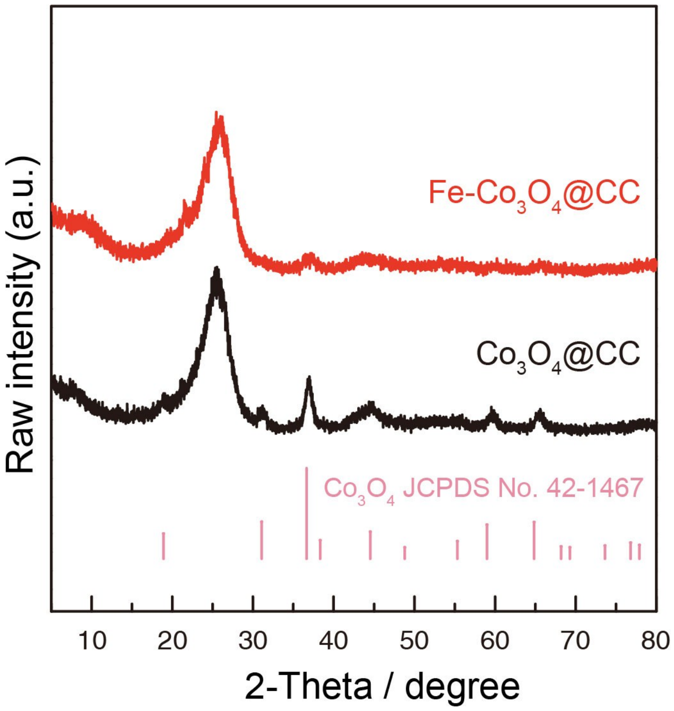

Fig. S1 XRD patterns of Co_3O_4@CC and Fe-Co_3O_4@CC. The pink vertical lines are indexed to the spinel phase Co_3O_4 (JCPDS No. 42-1467).

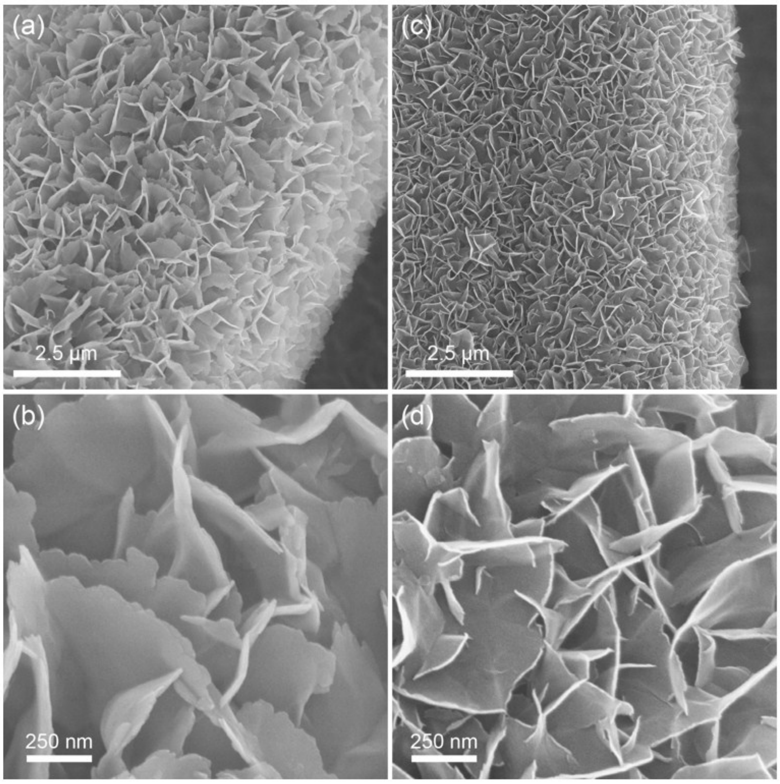

Fig. S2 SEM images of the precursors: (a-b) Co-LDH@CC and (c-d) CoFe-LDH@CC.

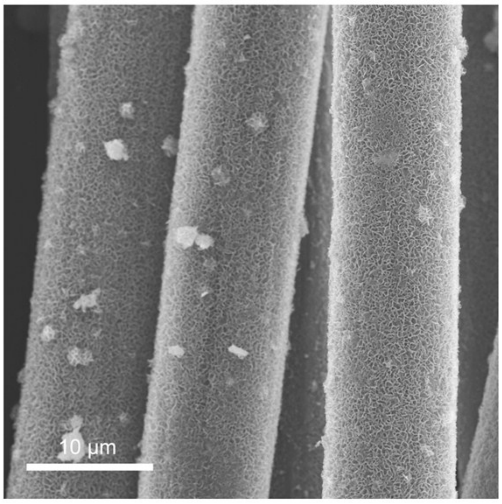

Fig. S3 The low-magnification SEM image of Fe-Co_3O_4@CC.

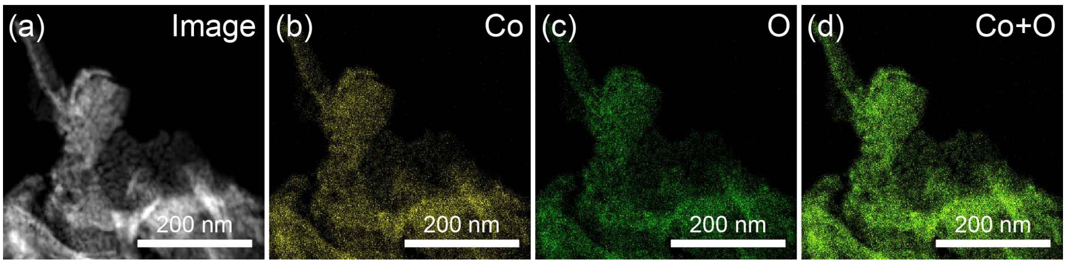

Fig. S4 EDS elemental mapping images of Co_3O_4 nanosheets peeled off from Co_3O_4@CC.

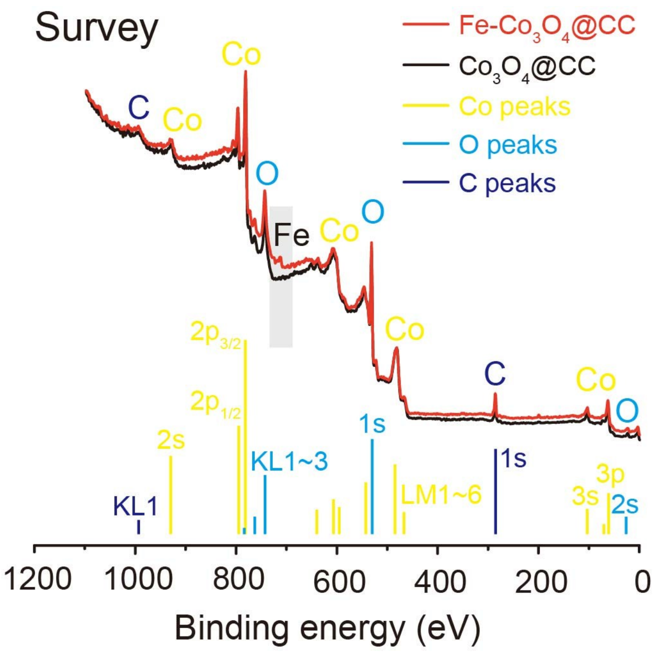

Fig. S5 The XPS survey spectra of the as-prepared Co_3O_4@CC and Fe-Co_3O_4@CC. Characteristic peak indicators for Co, O, and C are shown in yellow, cyan, and blue, respectively.

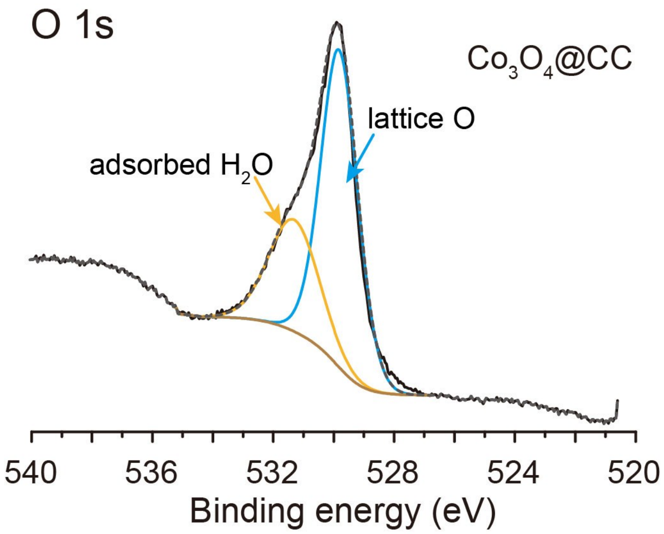

Fig. S6 XPS spectrum of O *1s* for Co_3O_4@CC.

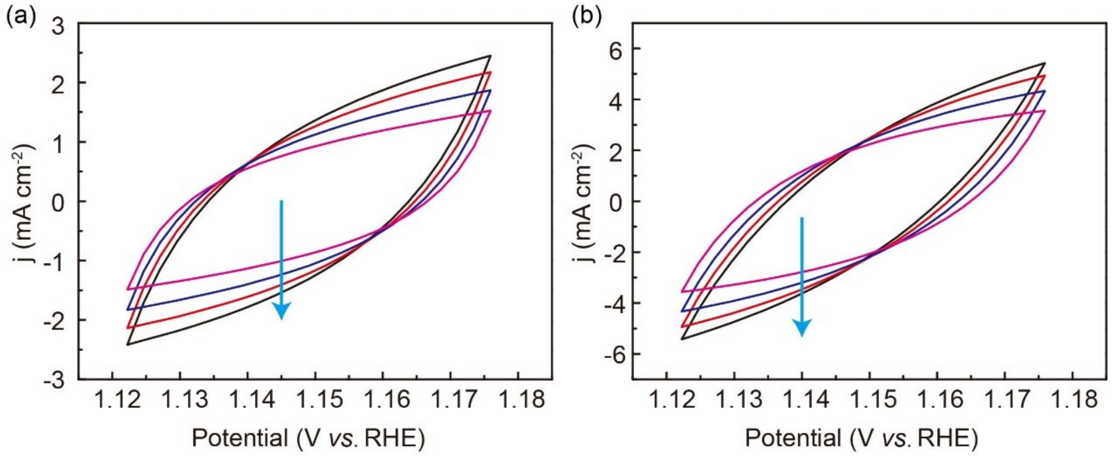

Fig. S7 Cyclic voltammograms at various scan rates of 40, 60, 80, 100, and 120 mV s^{-1} for (a) Co_3O_4@CC and (b) Fe-Co_3O_4@CC in 1 M KOH.

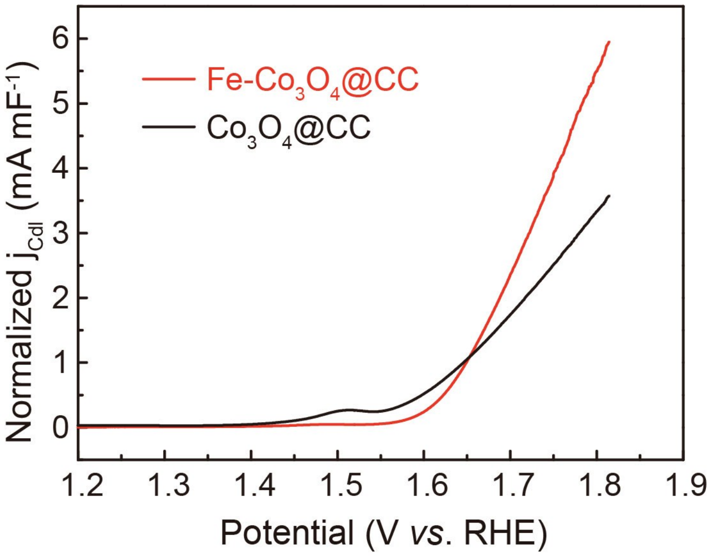

Fig. S8 OER polarization curves normalized by C_{dl} for Co_3O_4@CC and Fe-Co_3O_4@CC.

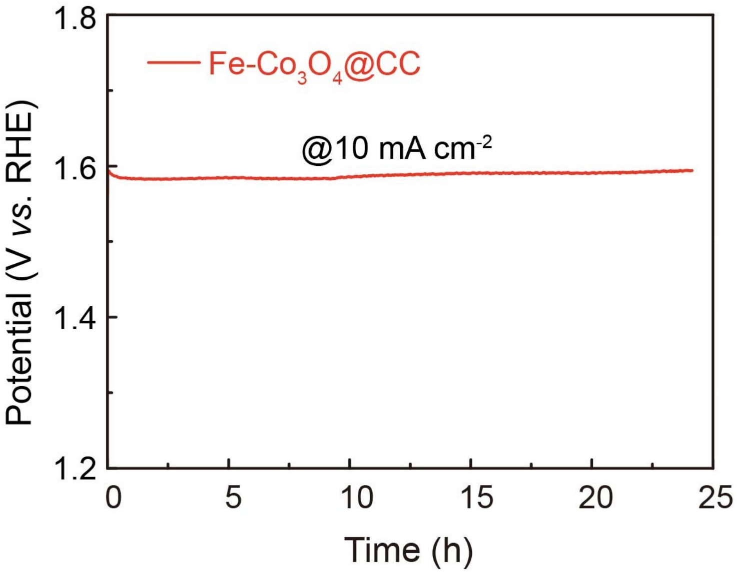

Fig. S9 Chronopotentiometric curves at a constant current density of 10 mA cm^{-2} of Fe-Co_3O_4@CC.

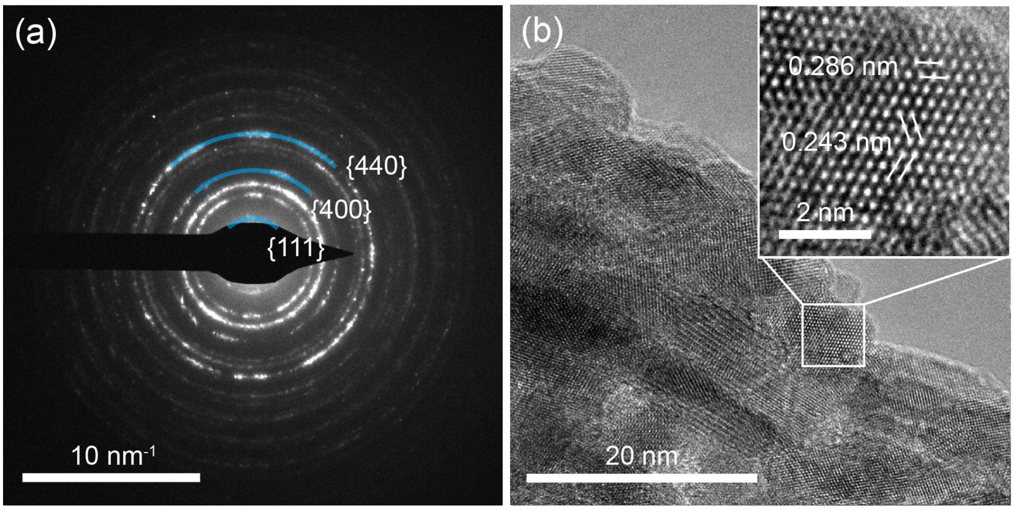

Fig. S10 (a) Selected area diffraction pattern of Fe-Co_3O_4@CC after the durability test. (b) HRTEM image of Fe-Co_3O_4@CC after the durability test, inset: enlarged HRTEM image.

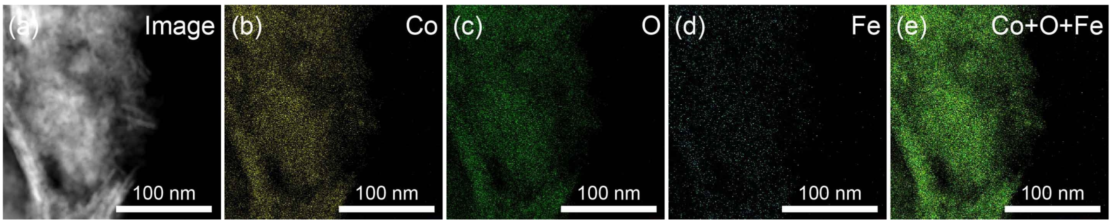

Fig. S11 EDS elemental mapping images of the Fe-Co_3O_4@CC after the durability test.

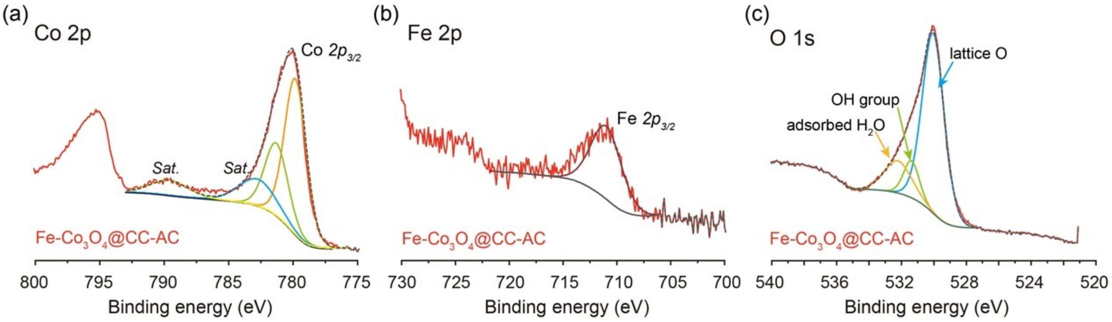

Fig. S12 XPS spectra of (a) Co 2p, (b) Fe 2p, and (c) O 1s for the Fe-Co_3O_4@CC after the durability test.

Table S1 Comparison of OER catalytic performance of various state-of-the-art electrocatalysts

Catalysts	Electrolyte	Overpotentials (mV) at		Tafel slope (mV dec^{-1})	References
		10 mA cm^{-2}	100 mA cm^{-2}		
Fe-Co_3O_4@CC	0.1 M KOH	388 mV (1.61V)	510 mV (1.74V)	72.6	This work
N-Co_3O_4 @NC-2	1 M KOH	266	-	54.9	Adv. Funct. Mater., 2019, 29, 1902875.
Co_3O_4@N-CNMAs /CC	1 M KOH	310	~ 460	58	Adv. Sci., 2019, 6, 1802243.
ultrafine Co_3O_4 (L-CO)	1 M KOH	271	~ 361	42	Adv. Funct. Mater., 2019, 29, 1903444.
Co_3O_4 /NPGC	0.1 M KOH	450	-	-	Angew. Chem. Int. Ed., 2016, 55, 4977.
Co_3O_4-NP /N-rGO	1 M KOH	380	~ 480	62	Adv. Energy Mater., 2017, 1702222.
Co_3O_4 NS/ZTC	1 M KOH	380	-	95	J. Mater. Chem. A, 2019, 7, 9988.
$P_{8.6}$-Co_3O_4/NF	1 M KOH	260@20	~ 315	60	ACS Catal., 2018, 8, 2236.
CoO /CoFeO	1 M KOH	297	370	61	Adv. Mater., 2018, 30, 1801211.
NF@PANI @$CoFe_2O_4$ /C NRAs	1 M KOH	240	~ 310	45	Adv. Mater., 2017, 29, 1604437.
CuNiN /FeNiCu	1 M KOH	300	400	45	Nat. Commun., 2018, 9, 2326.
NiCo@ $NiCoO_2$/C PMRAs	1 M KOH	366@20	420	84	Adv. Mater., 2018, 30, 1705442.
FCCH/NF	1 M KOH	228	252	42	Adv. Energy Mater., 2018, 8, 1800175.

Table S2 Comparison of ORR catalytic performance of various state-of-the-art electrocatalysts

Catalysts	Electrolyte	E_{onset} (V)	E_{half} (V)	Tafel slope (mV dec^{-1})	References
Fe-Co_3O_4@CC	0.1 M KOH	0.93	-	-	This work
N-Co_3O_4 @NC-2	0.1 M KOH	0.89	0.77	-	Adv. Funct. Mater., 2019, 29, 1902875.
Co/Co_3O_4@ PGS	0.1 M KOH	0.97	0.89	52.6	Adv. Energy Mater., 2018, 1702900.
Co_3O_4@N-CNMAs /CC	1 M KOH	0.97	0.90	68	Adv. Sci., 2019, 6, 1802243.
ultrafine Co_3O_4 (L-CO)	1 M KOH	0.936	0.878	47	Adv. Funct. Mater., 2019, 29, 1903444.
Co_3O_4 /NPGC	0.1 M KOH	0.97	0.842	-	Angew. Chem. Int. Ed., 2016, 55, 4977.
Co_3O_4-NP /N-rGO	0.1 M KOH	0.89	0.76	62	Adv. Energy Mater., 2017, 1702222.
Co@Co_3O_4 @NC-900	0.1 M KOH	-	0.80	-	J. Mater. Chem. A, 2018, 6, 1443.
Co_3O_4 NS/ZTC	0.1 M KOH	0.81	0.70	-	J. Mater. Chem. A, 2019, 7, 9988.
Co@Co_3O_4 /NC-2	0.1 M KOH	-	0.74	-	Angew. Chem. Int. Ed., 2016, 55, 4087.
Co_2FeO_4 /NCNT	0.1 M KOH	0.90	0.80	84.8	Angew. Chem. Int. Ed., 2019, 58, 13291.

Table S3 Comparison of Zinc-air battery performance using various state-of-the-art electrocatalysts.

Catalysts [electrolytes]	Power density (mW cm^{-2})	Stability details	References
Fe-Co_3O_4@CC [6 M KOH]	268.6	Stable ≥ 100 h @2 mA cm^{-2} (↑ 8 mV)	This work
N-Co_3O_4 @NC-2 [6 M KOH]	174.1	Stable ≥ 50 h @5 mA cm^{-2} (↑ 12 mV)	Adv. Funct. Mater., 2019, 29, 1902875.
Co/Co_3O_4 @PGS [6 M KOH]	118.27	Stable ≥ 800 h @10 mA cm^{-2} (↑ 50 mV)	Adv. Energy Mater., 2018, 1702900.
Co_3O_4@N-CNMAs/CC [6 M KOH]	75	Slight loss after 384 h @5 mA cm^{-2}	Adv. Sci., 2019, 6, 1802243.
ultrafine Co_3O_4 (L-CO) [6 M KOH]	337	Stable ≥ 180 h @2/20 mA cm^{-2} (↑ 48 mV)	Adv. Funct. Mater., 2019, 29, 1903444.
Co_3O_4/NPGC [6 M KOH]	-	Stable ≥ 80 h @5 mA cm^{-2} (↑ ~ 60 mV)	Angew. Chem. Int. Ed., 2016, 55, 4977.
Co_3O_4-NP /N-rGO [6 M KOH]	118	Slight loss after 16.7 h @5 mA cm^{-2}	Adv. Energy Mater., 2017, 1702222.
Co@Co_3O_4 @NC-900 [6 M KOH]	64	Stable ≥ 200 h @5 mA cm^{-2}	J. Mater. Chem. A, 2018, 6, 1443.
Co_3O_4 NS/ZTC	-	Stable ≥ 6 h @5 mA cm^{-2}	J. Mater. Chem. A, 2019, 7, 9988.
Co_2FeO_4 /NCNT [6 M KOH]	90.68	Slight loss after 8 h @30 mA cm^{-2}	Angew. Chem. Int. Ed., 2019, 58, 13291.